

Earlier work, based only on LFM, wrongly assigned the tilt direction (7).

What could explain the observed friction anisotropy? Traditional interpretations can be ruled out: Asperity interactions, plastic degradation, and adhesion hysteresis fail to account for it. We have found only one other system with behavior analogous to our anisotropy data: anisotropic viscosity in liquid crystals. Liquid crystals consist of rod-like molecules with a preferred orientation, and thus they bear certain similarities to the alkyl chains of our lipid monolayer (18). A few studies on the viscosities of nematic phases of liquid crystals have been published, and they report a consistent pattern of anisotropy: The coefficients of viscosity for flow perpendicular to the rod axis ("director") are higher than those for flow parallel to the director (19). This corresponds well with our measurements; we observed higher total friction (that is, energy dissipation) perpendicular to the tilt direction than parallel to the tilt direction.

We have as yet no explanation for the observed friction asymmetry. Why should there be less friction when scanning against the tilt direction than when scanning with it? We can only note that the energy dissipation is a collective property of the monolayer film and that it should depend (among other things) on the contact area between tip and surface and the tip penetration depth into the film. Perhaps a greater stiffness against the tilt direction reduces the penetration depth and thus the friction forces (20). More experimental and theoretical work on the viscoelastic properties of monolayers will be needed before we can understand the friction behavior observed in this study.

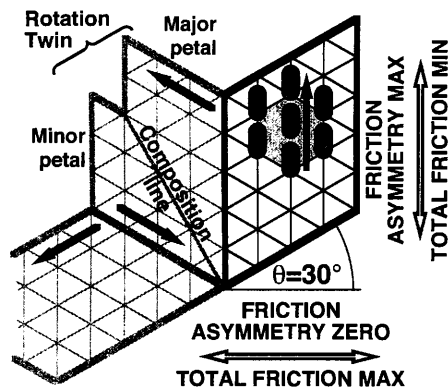


Fig. 3. Correlation of the friction force results (friction directions refer to the black petal) with the results obtained from structural analysis. The grid indicates the lattice directions of the subdomains as revealed by electron diffraction. Filled arrows represent the tilt direction of the alkyl chains as deduced from Brewster angle microscopy. The tilt direction of the minor petal is deduced from the $\sim 180^\circ$ phase difference of the friction asymmetry.

REFERENCES AND NOTES

1. D. Dowson, *History of Tribology* (Longman, London, 1979).
2. F. P. D. Bowden and D. Tabor, *Friction and Lubrication of Solids, Part I* (Oxford Univ. Press, Oxford, 1954).
3. H. Yoshizawa, Y.-L. Chen, J. Israelachvili, *J. Phys. Chem.* **97**, 4128 (1993).
4. M. Hirano, K. Shinjo, R. Kaneko, Y. Murata, *Phys. Rev. Lett.* **67**, 2642 (1991).
5. R. Overney, M. Fujihira, H. Takano, W. Paulus, H. Ringsdorf, *ibid.* **72**, 3546 (1994).
6. L. Santesson *et al.*, *J. Phys. Chem.* **99**, 1038 (1995).
7. D. Gourdon *et al.*, *Tribol. Lett.* **3**, 317 (1997).
8. We used the amphiphile bis[β -(1,2-dipalmitoyl-sn-glycero-3-phosphoryl)-3,6-dioxaoctyl] disulfide ("thio-lipid"), each molecule of which consists of two chiral phospholipids linked by a hydrophilic spacer.
9. H. Lang, C. Duschl, H. Vogel, *Langmuir* **10**, 197 (1994).
10. A. Ulman, *An Introduction to Ultrathin Organic Films: From Langmuir-Blodgett to Self-Assembly* (Academic Press, San Diego, CA, 1991).
11. Lateral force measurements based on optical lever detection were performed under ambient conditions on an M5 atomic force microscope (Park Scientific Instruments). We used V-shaped cantilevers (thickness, $\sim 0.6 \mu\text{m}$) with sharpened conical pure silicon tips and nominal normal and torsional spring constants of 0.03 and 1.2 N m^{-1} , respectively. The tip had a radius of curvature of 40 nm and an amorphous silicon oxide surface. The applied load and the adhesive force were each $\sim 5 \text{ nN}$.
12. The friction contrast is independent of the mica substrate. Similar results were obtained on silicon wafers with amorphous SiO_2 adlayers.
13. C. Giacomazzo, Ed., *Fundamentals of Crystallography* (Oxford Univ. Press, Oxford, 1992), p. 83.
14. U. D. Schwarz, H. Bluhm, H. Hölscher, W. Allers, R. Wiesendanger, in *The Physics of Sliding Friction*, B. N. J. Persson and E. Tosatti, Eds. (Kluwer Academic, Dordrecht, Netherlands, 1996), pp. 369–402.
15. A. Fischer and E. Sackmann, *Nature* **313**, 299 (1985).
16. D. Hönig and D. Möbius, *J. Phys. Chem.* **95**, 4590 (1991).
17. C. Lautz, J. Kildae, T. M. Fischer, *J. Chem. Phys.* **106**, 7448 (1997).
18. We estimate that the tip penetrates $\sim 5 \text{ \AA}$ into the lipid monolayer domains, which have a thickness of 25 \AA .
19. S. Chandrasekhar, *Liquid Crystals* (Cambridge Univ. Press, Cambridge, 1992).
20. R. M. Overney *et al.*, *Langmuir* **10**, 1281 (1994).
21. Brewster angle microscopy could not be used to characterize the lipid layers on mica because it is an unsuitable substrate for optical reflection techniques.
22. Supported by the Swiss National Research Foundation (NFP 36: 4036-044084/1), SPP Biotechnology, and the board of the Swiss Federal Institutes of Technology (SPP MINAST, 7.06).

17 November 1997; accepted 17 February 1998

Generation of Intestinal T Cells from Progenitors Residing in Gut Cryptopatches

Hisashi Saito, Yutaka Kanamori, Toshitada Takemori, Hideo Nariuchi, Eiro Kubota, Hiromi Takahashi-Iwanaga, Toshihiko Iwanaga, Hiromichi Ishikawa*

Cryptopatches (CPs) are part of the murine intestinal immune compartment. Cells isolated from CPs of the small intestine that were c-kit positive (c-kit⁺) but lineage markers negative (Lin⁻) gave rise to T cell receptor (TCR) $\alpha\beta$ and TCR $\gamma\delta$ intestinal intraepithelial T cells after in vivo transfer or tissue engraftment into severe combined immunodeficient mice. In contrast, cells from Peyer's patches and mesenteric lymph nodes, which belong in the same intestinal immune compartment but lack c-kit⁺Lin⁻ cells, failed to do so. These findings and results of electron microscopic analysis provide evidence of a local intestinal T cell precursor that develops in the CPs.

The gastrointestinal mucosa is one of the largest interfaces in the body with only a single layer of epithelium separating the

exposed external lumen from the internal milieu, and in primitive vertebrates, only gut-associated lymphoid tissues are present (1). Therefore, from an evolutionary perspective, it is possible that the intestinal tract of higher vertebrates retains some self-supporting immune system to ensure internal integrity (2). The numerous intestinal intraepithelial T cells (IELs) have cellular and behavioral characteristics distinct from those of other peripheral T cells (2–6) and are enriched with TCR $\gamma\delta$ T cells (7). In mice, most TCR $\gamma\delta$ IELs and many TCR $\alpha\beta$ IELs, unlike blood-borne T cells, use the CD8 $\alpha\alpha$ homodimer (2, 8) instead of CD8 $\alpha\beta$ and develop somewhere in the intestinal mucosa without passing through the thymus (2, 4, 8, 9).

H. Saito, Y. Kanamori, H. Ishikawa, Department of Microbiology, Keio University School of Medicine, Tokyo 160, Japan.

T. Takemori, Department of Immunology, National Institute of Infectious Diseases, Tokyo 162, Japan.

H. Nariuchi, Department of Allergology, Institute of Medical Science, University of Tokyo, Tokyo 108, Japan.

E. Kubota, Second Department of Oral and Maxillofacial Surgery, Kanagawa Dental College, Kanagawa 238, Japan.

H. Takahashi-Iwanaga, Department of Anatomy, School of Medicine, Hokkaido University, Sapporo 060, Japan.

T. Iwanaga, Laboratory of Anatomy, Graduate School of Veterinary Medicine, Hokkaido University, Sapporo 060, Japan.

*To whom correspondence should be addressed. E-mail: ishikawa@sun.microb.med.keio.ac.jp

Our immunohistochemical search (10) for anatomical sites of IEL generation revealed multiple tiny clusters [the cryptopatches (CPs)] filled with ~ 1000 c-kit⁺IL-7R⁺Thy1⁺ lymphohematopoietic cells in the lamina propria (LP) of the murine intestinal crypt. The presence of this phenotype suggested that the cells of the CPs could be T lineage-committed precursors (10). CP cells are widely distributed in small numbers throughout the length of the intestine (10) and are visible stereomicroscopically from the serosa, although in our study this was strain dependent—for example, observation was easiest in BALB/c mice (Fig. 1A) and most difficult in C57BL/6 mice. Subsequently, we isolated tiny fragments of the small intestine

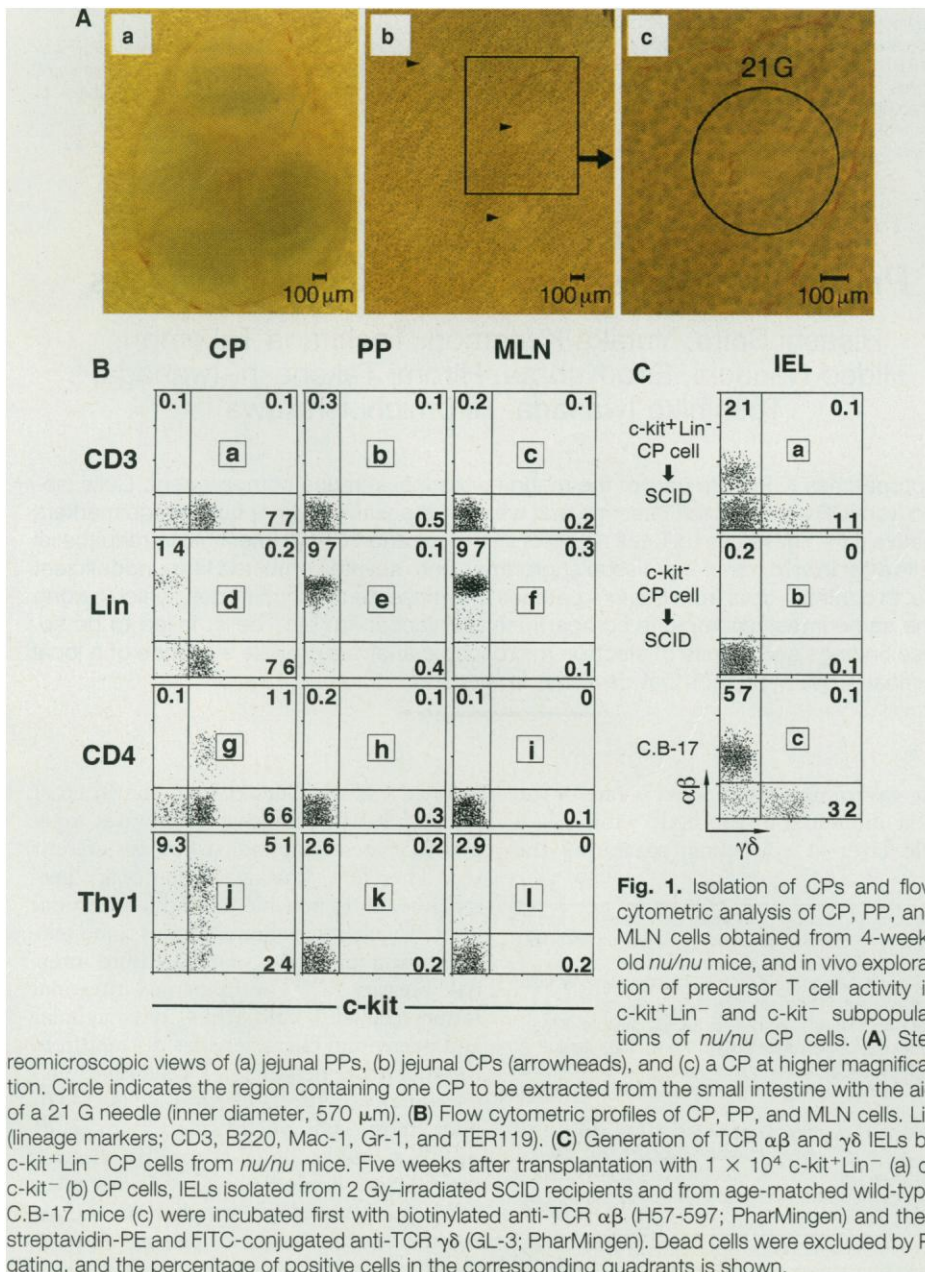
(~ 0.13 mm³) containing one CP using an amputated and tapered 21 G needle (Fig. 1A). In one such fragment containing a CP and a fragment extracted from the region without CPs, we detected 1000 (range, 650 to 2000) and 60 (range, 25 to 150) lymphoid cells, respectively.

We analyzed CP, PP (Peyer's patch), and MLN (mesenteric lymph node) cells obtained from 4-week-old athymic (*nu/nu*) weanling BALB/c mice by flow cytometry (11). All locations had no CD3⁺ T cells (Fig. 1B) or CD8⁺ cells, and most CP cells were c-kit⁺Lin⁻ (Lin; CD3, B220, Mac-1, Gr-1, and TER119) (Fig. 1B), whereas cells from PPs and MLNs (Fig. 1B), and cells from the tissue fragments without CPs, did not have a c-kit⁺Lin⁻ popula-

tion. Almost all c-kit⁺Lin⁻ CP cells were IL-7R⁺Pgp-1⁺ (12), 14% of c-kit⁺Lin⁻ CP cells were CD4⁺ (Fig. 1B), and 68% of c-kit⁺Lin⁻ CP cells were Thy1⁺ (Fig. 1B). Four distinct lymphocyte subsets were present among c-kit⁺Lin⁻ CP cells as determined by the expression of CD4 and Thy1. In the three lymphoid tissues of euthymic *nu/+* littermates, only CP cells contained a dominant population (60 to 70%) of c-kit⁺Lin⁻ cells (12). Thus, CPs differed from PPs and MLNs with respect to lymphoid residents, although they all constitute organized gut-associated lymphoid tissue (GALT).

To determine whether progenitors for intestinal T cells are present in CP cells from *nu/nu* mice, we transplanted intravenously 10,000 c-kit⁺Lin⁻ or c-kit⁻ CP cells (Fig. 1B), sorted by flow cytometry, into 2 gray (Gy)-irradiated C.B-17/severe combined immunodeficient (SCID) mice (13) (Fig. 1C). The c-kit⁺Lin⁻ cells but not c-kit⁻ cells were able to generate $\alpha\beta$ and $\gamma\delta$ T cells in the IEL compartment. The c-kit⁺Lin⁻ cells also gave rise to substantial $\alpha\beta$ T cells in MLNs and to a lesser extent in the spleen and thymus, but were unable to reconstitute B cells in any of the recipient's lymphoid tissues (see below). For a more comprehensive transplantation study on c-kit⁺Lin⁻ CP cells, we used the whole CP cell population, rather than sorted c-kit⁺Lin⁻ cells, because considerable time was required for isolation of CP cells, and the subsequent procedure of cell fractionation often resulted in unforeseeable impairment of cell viability.

For this purpose, 5×10^4 CP, PP, or MLN cells obtained from 4-week-old *nu/nu* mice (Fig. 1B) were transplanted intravenously into 2 Gy-irradiated SCID mice, because of the extremely small number of mature CD3⁺ T cells (Fig. 1B) that could expand and survive for extended periods in immunodeficient recipient mice (14). Three weeks after transplantation, CP cells generated T cells in the IEL and MLN compartments (Fig. 2, A to C) but few in the spleen and thymus compartments (Fig. 2, A and C). Absolute numbers of T cells recovered from these anatomical sites reached 3×10^6 to $\sim 4 \times 10^6$, indicating that repopulation of T cells by CP cells accompanied cell proliferation. CP cells gave rise to $\alpha\beta$ T cells in both the IEL and MLN compartments, but to $\gamma\delta$ T cells only in the IEL compartment (Fig. 2B). The relative proportions of CD8 α^+ to CD8 β^+ and of CD8 α^+ to CD8 β^+ cells in the reconstituted MLNs were 6 to 18 and 1.1 to 1.3, respectively. The collective reconstitution of T cells from CP cells in the posttransplantation time frame was quantitated (Fig. 2C). However, CP cells were unable to



generate B220⁺ or sIgM⁺ B cells (Fig. 2A), and cells from PPs (Fig. 2A, third column) and MLNs (Fig. 2A, fourth column) that lacked the c-kit⁺Lin⁻ subset (Fig. 1B) did not fill the empty T and B cell compartments as of 7 weeks after transplantation (12), indicating that the relevant T lineage-committed precursors in CPs are indeed c-kit⁺Lin⁻ cells.

It is conceivable that B cell (Fig. 2A) and probably myeloid cell progenitors are minimal, if present at all, in CP cells and that T cell progeny of c-kit⁺Lin⁻ CP cells actually develop in the extrathymic site (or sites) because intestinal epithelium and MLNs are already colonized with T cells 2 weeks after transplantation, although, at this time, T cells are absent in the recipient's thymus (Fig. 2C). Our preliminary *in vitro* study confirmed that sorted c-kit⁺Lin⁻ cells from CPs failed to generate not only B and myeloid cell colonies in cultures on a monolayer of a fetal thymus-derived stromal cell line TSt-4 (15) but also T cells in deoxyguanosine-treated fetal thymus lobes in a high-oxygen submersion (HOS) organ culture (15). In contrast, this was not true of those from fetal liver and adult bone marrow.

Next, we engrafted 10 tissue fragments extracted from the small intestine of weanling *nu/nu* mice with or without CPs (Fig. 1A) into the kidney capsule of unirradiated SCID mice. Consistent with the observation in the cell transplantation study, engraftment of CP⁺ but not CP⁻ fragments resulted in the emergence of T cells in the recipient's intestine and MLNs. Five weeks after engraftment, CD3⁺ T cells were generated in the villus epithelium (IELs) and to a lesser extent in the villus LP (Fig. 3A). There were, however, marked differences between implanted (Fig. 3, C and D) and *in situ* (10) CPs. (i) The cellular mass of implanted CPs was enlarged about two- to threefold in diameter (Fig. 3, C and D) compared with that of *in situ* CPs (10). (ii) A substantial number of CD3⁺ T cells were detected in the central region of implanted CPs (Fig. 3C), but few were detected in *in situ* CPs (Fig. 1B) (10). (iii) c-kit⁺ cells found at high density throughout the *in situ* CPs (10) were compartmentalized in the peripheral region of implanted and enlarged CPs (Fig. 3D). Therefore, extraintestinal administration of c-kit⁺Lin⁻ CP cells by tissue engraftment and intravenous transplantation *per se* appears to be responsible for the generation of T cells in the ectopic anatomical sites (Figs. 2 and 3) as well as in the entopic intestinal mucosa. Mosley and Klein (16) reported that ectopic engraftment of fetal intestine in the kidney capsule of athymic recipient mice pro-

notes the generation of peripheral T cells, whereas peripheral lymphoid tissues lack T cells in sham-engrafted athymic mice

although they have their own intestine. Electron microscopy (17) showed that numerous lymphocytes cross the basement

Fig. 2. CP but not PP and MLN cells isolated from 4-week-old *nu/nu* mice generate T cells *in vivo* after intravenous transplantation into 2 Gy-irradiated SCID mice. (A) Three weeks after transplantation with 5×10^4 CP, PP, or MLN cells, IELs and MLN, spleen, and thymus cells isolated from the corresponding 2 Gy-irradiated recipient mice, from 2 Gy-irradiated sham-transplanted SCID mice (negative control), and from age-matched C.B-17 mice (positive control) were incubated first with biotinylated anti-CD3 and then with streptavidin-PE and FITC-conjugated anti-B220. Dead cells were excluded by PI gating. FACScan profiles of inguinal LN cells isolated from the same SCID recipients of CP cells were comparable with those of MLN cells shown in this figure. A substantial number of IELs (first row) were B220 dull positive as reported elsewhere (21), but they were cell surface sIgM⁻ (72). (B) Three weeks after transplantation with 5×10^4 CP cells, IELs and MLN cells isolated from the SCID recipients and from age-matched C.B-17 mice (positive control) were incubated first with biotinylated anti-TCR $\alpha\beta$ and then with streptavidin-PE and FITC-conjugated anti-TCR $\gamma\delta$. Dead cells were excluded by PI gating. (C) Reconstitution of T cells in IEL (○), MLN (●), spleen (□), and thymus (■) compartments of 2 Gy-irradiated SCID recipients transplanted with 5×10^4 CP cells from 4-week-old *nu/nu* mice. The data are shown as the mean \pm SD of four independent experiments with three to five SCID mice per analysis.

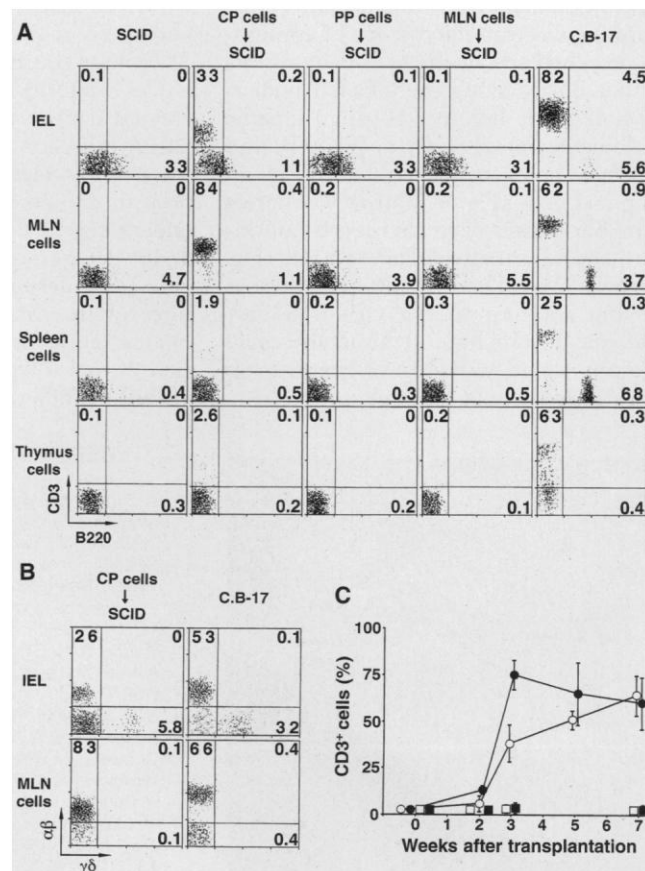
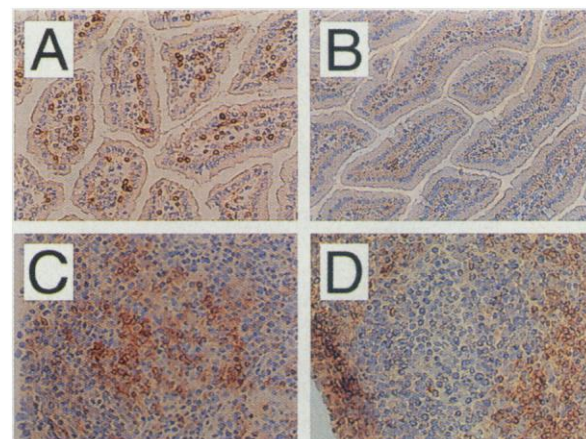


Fig. 3. Generation of T cells in the intestinal villi of SCID mice after engraftment of tissue fragments containing CPs. SCID mice were engrafted by bilateral implantation under the kidney capsule with 10 tiny tissue fragments (~0.13 mm³ per fragment) with or without CP (Fig. 1A) extracted from the small intestine of 4-week-old *nu/nu* mice. Five weeks after engraftment, immunohistochemical analysis of fresh cryosections prepared from the recipient's small intestine and kidneys containing implanted CPs was carried out as described (10). (A) CD3⁺ T cells were generated extensively in the intestinal epithelia of SCID mice engrafted with the CP⁺ tissue fragments (magnification, $\times 200$). A limited number of T cells were also located in the LP. (B) CD3⁺ T cells were not generated in the intestinal villi of SCID mice engrafted with CP⁻ tissue fragments ($\times 200$). Immunohistochemical visualization of (C) CD3⁺ and (D) c-kit⁺ cells in two consecutive tissue sections of a representative CP graft ($\times 200$). (C) CD3⁺ T cells were generated in the central region and (D) c-kit⁺ cells were compartmentalized in the peripheral region of an implanted CP graft, respectively.



membrane (Bm) that comes in contact with the CPs (Fig. 4A) and that a large number of lymphocytes are present in the epithelium adjacent to the CPs as compared with the epithelium of the villi and crypts (12). Scanning electron microscopy of epithelium-detached specimens (18) demonstrated that Bm covering the CPs has numerous holes (one hole per 10 μm^2) ranging in diameter from 3 to 6 μm (Fig. 4B) and that these holes are often filled with round lymphoid cells (Fig. 4C, arrows), whereas crypt Bm creates deep cavities, is continuous, and is virtually devoid of holes (Fig. 4B, asterisks). These results suggest that the Bm adjacent to the CPs is a busy anatomical front line of the mouse small intestine where migration of lymphocytes into the epithelium takes place.

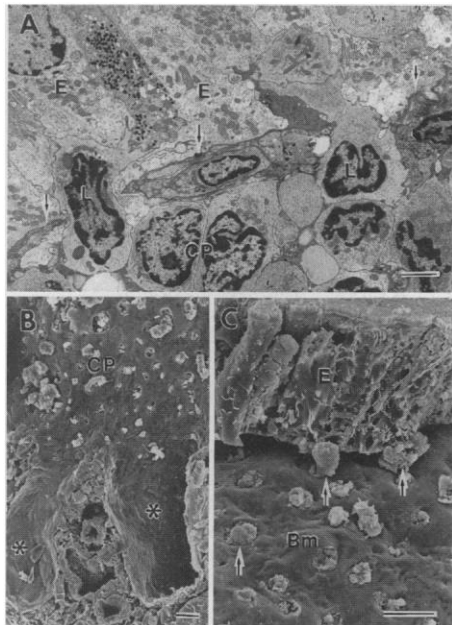


Fig. 4. Electron microscopic analysis of the epithelium adjacent to CPs and the basement membrane (Bm) covering CPs. **(A)** Electron micrograph showing a peripheral region of a cryptopatch (CP) facing the epithelium (E). Two lymphocytes (L) are passing through the Bm (arrows). Bar, 2 μm . **(B)** Scanning electron micrograph of epithelium-detached Bm extending over a CP. Numerous holes, which probably facilitate the migration of CP lymphocytes into the epithelium, are apparent. No such holes occur in the Bm of the cryptal region (asterisks). Bar, 10 μm . Although not shown, epithelial Bm encompassing villous LP also contains a substantial number of holes, which are usually no larger than 1 μm in diameter, and no cellular elements plug the smaller holes. **(C)** Scanning electron micrograph showing a peripheral region of a CP covered by Bm. Part of the epithelium (E) has been detached from the specimen exposing the highly perforated Bm. Lymphocytes in a CP have balloon-shaped cytoplasmic processes protruding through these holes into the epithelium (arrows). Bar, 10 μm .

On the basis of the cellular, functional, and structural properties described above, CPs fulfill the criteria for lymphoid tissues wherein precursor IELs develop. The ability of the intestine to induce T cell lymphopoiesis makes phylogenetic sense (1, 2) because the enteric mucous membrane is the locale in the body exposed to the greatest danger, and it is here that external antigens continually enter the body. In this context, identification of CPs will not only shed light on the intestinal events underlying the development of IELs (2–6, 8, 9, 19) but may also offer additional clues for understanding the distinctive features of intestinal immune responses to luminal antigens (20) such as the induction of oral tolerance and immunopathogenesis of inflammatory bowel disease.

REFERENCES AND NOTES

1. A. Zapata, *Bull. Inst. Pasteur* **81**, 165 (1983); S. Tomonaga, T. Hirokame, K. Awaka, *Zool. Mag.* **82**, 215 (1973); L. D. Pasquier, in *Evolution of the Immune System, Fundamental Immunology*, W. E. Paul, Ed. (Raven, New York, 1993), pp. 199–233.
2. L. Lefrancois and L. Puddington, *Immunol. Today* **16**, 16 (1995); J. R. Klein, *J. Exp. Med.* **184**, 1203 (1996); G.-K. Sim, *Adv. Immunol.* **58**, 297 (1995); A. M. Mowat and J. L. Viney, *Immunol. Rev.* **156**, 145 (1997).
3. S. P. Balk *et al.*, *Science* **253**, 1411 (1991); C. Van Kerckhove *et al.*, *J. Exp. Med.* **175**, 57 (1992); Y. Chowder, W. Holtmeier, J. Harwood, E. Morzycka-Wroblewska, M. F. Kagnoff, *ibid.* **180**, 183 (1994); A. Regnault *et al.*, *Eur. J. Immunol.* **26**, 914 (1996).
4. M. Malissen *et al.*, *EMBO J.* **12**, 4347 (1993); C. Liu *et al.*, *ibid.*, p. 4863; S. Y. Park *et al.*, *Eur. J. Immunol.* **25**, 2107 (1995).
5. N. Cerf-Bensussan *et al.*, *Eur. J. Immunol.* **17**, 1279 (1987); K. L. Cepek *et al.*, *Nature* **372**, 190 (1994).
6. B. Rocha, P. Vassalli, D. Guy-Grand, *J. Exp. Med.* **173**, 483 (1991); P. Poussier, H. S. Teh, M. Julius, *ibid.* **178**, 1947 (1993); S. R. Guehler, J. A. Bluestone, T. A. Barrett, *ibid.* **184**, 493 (1996).
7. T. Goodman and L. Lefrancois, *Nature* **333**, 855 (1988); M. Bonneville *et al.*, *ibid.* **336**, 479 (1988); K. Deusch *et al.*, *Eur. J. Immunol.* **21**, 1053 (1991); S. Porcelli, M. B. Brenner, H. Band, *Immunol. Rev.* **120**, 137 (1991); H. Komano *et al.*, *Proc. Natl. Acad. Sci. U.S.A.* **92**, 6147 (1995); K. Fujihashi *et al.*, *J. Exp. Med.* **183**, 1929 (1996).
8. D. Guy-Grand *et al.*, *J. Exp. Med.* **173**, 471 (1991); L. Lefrancois, *J. Immunol.* **147**, 1746 (1991); P. Poussier, P. Edouard, C. Lee, M. Binnie, M. Julius, *J. Exp. Med.* **176**, 187 (1992).
9. J. R. Klein, *J. Exp. Med.* **164**, 309 (1986); L. Lefrancois, R. LeCorre, J. Mayo, J. A. Bluestone, T. Goodman, *Cell* **63**, 333 (1990); A. Bandeira *et al.*, *Proc. Natl. Acad. Sci. U.S.A.* **88**, 43 (1991); B. Rocha, P. Vassalli, D. Guy-Grand, *J. Exp. Med.* **180**, 681 (1994).
10. Y. Kanamori *et al.*, *J. Exp. Med.* **184**, 1449 (1996).
11. CP, PP, and MLN cells obtained from two 4-week-old athymic (*nu/nu*) BALB/c mice (CLEA Japan, Tokyo, Japan) were incubated first either with biotinylated monoclonal antibody (mAb) to CD3 (anti-CD3) (2C11; PharMingen), biotinylated mAbs to lineage (anti-lineage) markers (Lin; CD3, B220, Mac-1, Gr-1, and TER119), biotinylated anti-CD4 (RM4-5; PharMingen), biotinylated anti-Thy1.2 (30-H 12; PharMingen), or biotinylated anti-CD8 α (53-6.7; PharMingen), followed by incubation with streptavidin-phycoerythrin (PE) (Becton Dickinson) and fluorescein isothiocyanate (FITC)-conjugated anti-c-kit (ACK-4). CP cells were also incubated first either with biotinylated anti-IL-7R (A7R34) or biotinylated anti-Pgp-1 (IM7; PharMingen) and then with streptavidin-PE and FITC-conjugated anti-c-kit. Anti-B220 (RA3-6B2), anti-Mac-1 (M1/70) and anti-Gr-1 (RB6-8C7), and mAb TER-119 were from PharMingen. Stained cells were suspended in staining medium (Hanks solution without phenol red, 0.02% NaN_3 , and 2% heat-inactivated fetal bovine serum) containing propidium iodide (PI, 0.5 $\mu\text{g}/\text{ml}$) and analyzed by FACScan with LYSYSII software (Becton Dickinson). Dead cells were excluded by PI gating. For three-color analysis, CP cells were incubated first with biotinylated anti-Thy1.2 and then with streptavidin-Tri-Color (Caltag), FITC-conjugated anti-c-kit, and PE-conjugated anti-CD4 (RM4-5; PharMingen). Cells were incubated with anti-Fc γ II/III (2.4G2; PharMingen) before staining to block nonspecific binding of labeled mAbs to FcR.
12. H. Saito *et al.*, data not shown.
13. About 5×10^5 CP cells of 4-week-old *nu/nu* mice that had been isolated from 500 tissue fragments of the small intestine containing one CP were stained with FITC-conjugated anti-lineage mAbs and biotinylated anti-c-kit mAb plus streptavidin-PE. Stained cells were analyzed by FACScan, and then c-kit⁺ Lin⁻ and c-kit⁻ subpopulations were sorted by FACS Vantage (Becton Dickinson). Sorted cells were reanalyzed to determine their purity and were found to be >98% pure. Finally, 10,000 sorted c-kit⁺ Lin⁻ or c-kit⁻ cells were transplanted intravenously into 4 to 6 C.B-17/SCID mice (CLEA Japan) that had been irradiated 5 to 7 hours previously with 2 Gy from an x-ray source. Three to 7 weeks after transplantation, cells isolated from the recipient's lymphoid tissues were analyzed by flow cytometry.
14. J. Sprent, M. Schaefer, M. Hurd, C. Surh, Y. Ron, *J. Exp. Med.* **174**, 717 (1991); S. Takeda, H.-R. Rodewald, H. Arakawa, H. Bluethmann, T. Shimizu, *Immunity* **5**, 217 (1996).
15. H. Kawamoto, K. Ohmura, Y. Katsura, *Int. Immunol.* **9**, 1011 (1997).
16. R. L. Mosley and J. R. Klein, *J. Exp. Med.* **176**, 1365 (1992).
17. Tiny tissue fragments each containing one CP were extracted from the small intestine of BALB/c mice under a stereomicroscope and fixed for 2 hours in 2.5% glutaraldehyde buffered with 0.1 M phosphate (pH 7.4). After postfixation in 1% OsO_4 for 2 hours, the specimens were embedded in Epon 812. Ultrathin sections were observed with an H-7000 transmission electron microscope.
18. The small intestine of a BALB/c mouse was perfusion-fixed with a mixture containing 1.25% glutaraldehyde and 1% paraformaldehyde in 0.1 M phosphate buffer (pH 7.4). Small pieces of the tissue fragment containing one CP were prepared and macerated with 0.1% OsO_4 for 48 hours at 20°C. The specimens were postfixated with 1% tannic acid followed by 1% OsO_4 , critical-point dried, and metal-coated. A Hitachi S-4500 scanning electron microscope was used for observation.
19. J. W. Huleatt and L. Lefrancois, *Immunity* **5**, 263 (1996); J. Wang, M. Whetsell, J. R. Klein, *Science* **275**, 1937 (1997); F. Shanahan, *ibid.*, p. 1897.
20. W. Strober *et al.*, *Immunol. Today* **18**, 61 (1997); H. L. Weiner, *Annu. Rev. Med.* **48**, 341 (1997); M. F. Kagnoff, *Immunol. Today* **17**, 57 (1996); A. Mizoguchi, E. Mizoguchi, C. Chiba, A. T. Bhan, *J. Exp. Med.* **184**, 707 (1996); R. Aranda *et al.*, *J. Immunol.* **158**, 3464 (1997).
21. T. A. Barrett *et al.*, *J. Immunol.* **149**, 1124 (1992); T. Lin *et al.*, *Eur. J. Immunol.* **24**, 1080 (1994).
22. Animal care was in accordance with our institutional guidelines. We thank S. I. Nishikawa (Kyoto University) for mAb ACK-4 and T. Sudo (Toray Industries) for mAb A7R34; J. R. Klein for discussions; S. I. Nishikawa, L. Lefrancois, M. Nanno, S. Koyasu, H. Nagura, H. Kiyono, and Y. Katsura for comments and encouragement; and K. Ishimaru for technical assistance. Supported by the Agency of Science and Technology, Japan; by the Japan Society for the Promotion of Science (JSPS-RFTF 97L0071); and by a Waksman Foundation Award.

16 October 1997; accepted 5 March 1998